Exact solution for the time evolution of network rewiring models

T. S. Evans and A. D. K. Plato
Theoretical Physics, Blackett Laboratory, Imperial College London, London, SW7 2AZ, United Kingdom
(Received 1 September 2006; published 2 May 2007)

We consider the rewiring of a bipartite graph using a mixture of random and preferential attachment. The full mean-field equations for the degree distribution and its generating function are given. The exact solution of these equations for all finite parameter values at any time is found in terms of standard functions. It is demonstrated that these solutions are an excellent fit to numerical simulations of the model. We discuss the relationship between our model and several others in the literature, including examples of urn, backgammon, and balls-in-boxes models, the Watts and Strogatz rewiring problem, and some models of zero range processes. Our model is also equivalent to those used in various applications including cultural transmission, family name and gene frequencies, glasses, and wealth distributions. Finally some Voter models and an example of a minority game also show features described by our model.

DOI: 10.1103/PhysRevE.75.056101 PACS number(s): 89.75.Hc, 89.75.Da, 89.65.Ef, 89.65.Gh

I. INTRODUCTION

One of the most important classes of complex network models are those with a constant number of edges which evolve by rewiring those edges. The classic example of Watts and Strogatz [1] is of this type and such models are often studied in their own right [2–7]. Network rewiring is also related to some multiurn models [8–11] which include what are termed backgammon or balls-in-boxes models [12] used for glasses [13,14], simplicial gravity [15], and wealth distributions [16]. Models of the zero range process [17–19] are also closely linked. Since most practical systems cannot grow indefinitely networks of constant size have many applications: the transmission of cultural artifacts such as pottery designs, dog breed, and baby name popularity [20–25], the distribution of family names in constant populations [26], and the diversity of genes [27,28]. Aspects of the Voter model [29,30], as used to describe the competition between languages [31], and the popularity of minority game strategies [32] may also be cast in terms of network rewiring.

Analytic results for network models are limited. A typical approach starts from the master equations for the evolution of the degree distribution, these are given in a mean-field approximation in which the quantities are the average values of many possible realizations. Luckily in most models, and even in some real-world applications, the results from mean-field equations often agree extremely well with numerical simulations of the model.

Despite the simplifications brought by the mean-field approximation, the equations remain difficult to solve and it is normal to study the large graph and long time limit, e.g., see [33,34]. For instance, the finite size and/or time corrections to growing graphs using linear degree attachment probabilities are complicated and known only as an asymptotic expansion, for example, see [35,36]. In fact one of the most tractable examples remains the Erdős-Réyni random graph which can be seen as the long time limit of the Watts and Strogatz rewiring model [1].

What we show in this paper is that the mean field equations for the degree distribution of nongrowing rewiring models with linear rewiring probabilities can be solved *exactly* for *any* time. This goes beyond the results found in the literature (typically exact only for infinitely large systems in equilibrium) and extends the initial work on exact results in such models at equilibrium [37] and the preliminary non-equilibrium results of [38].

We start by setting up the model and the mean-field master equations for the degree distribution in the next section. We solve these in terms of the generating function in Sec. III and from this we consider the degree distribution in Sec. IV and then its moments in Sec. V. All this is done in terms of our simple network rewiring model but in Sec. VI we consider the relation between this model and a variety of other abstract models (with and without explicit networks) and various real world examples. Finally we summarize our conclusions and add some observations on how such preferential attachment may arise naturally and the scaling properties of our model.

II. THE MODEL

We will focus on a generic rewiring problem, which we shall describe in terms of a bipartite graph of E "individual" vertices, each having one edge fixed to any one of N "artifact" vertices, as shown in Fig. 1. Our naming of the vertices reflects our previous work and one possible application (cultural transmission) but apart from the names we will keep our presentation abstract until Sec. VI.

Each individual vertex is always connected to exactly one edge while the other end of each edge is connected to any artifact. The network changes by rewiring the artifact end of these edges and we will focus on the degree distribution of the artifact vertices at any one time, $n(k,t)$, and its probability distribution $p(k,t)=n(k,t)/N$, where k is the degree of an artifact vertex.

To make progress we make further simplifying assumptions. First we will assume that the population of individuals is absolutely constant so E is fixed and finite. Almost all other comparable work uses a large E approximation. We will also assume that the artifact choices available are fixed to be N so the average degree of an artifact vertex is $\langle k \rangle$

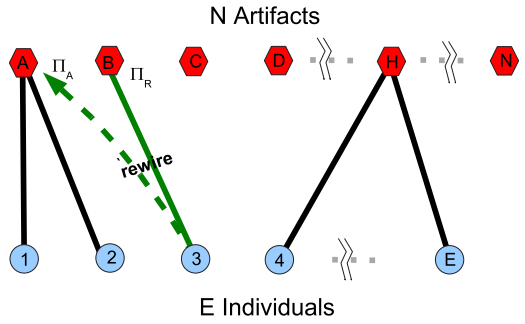

FIG. 1. (Color online) The bipartite graph has E individual vertices, each with one edge. The other end of the edge is connected to one of N artifact vertices. If the degree of an artifact vertex is k then this artifact has been "chosen" by k distinct individuals. At each time step a single rewiring of the artifact end of one edge occurs. An individual is chosen (number 3 here) with probability Π_R which gives us the departure artifact (here B). At the same time the arrival artifact is chosen with probability Π_A (here labeled A). After both choices have been made the rewiring is performed (here individual 3 switches its edge from artifact B to A).

$=E/N$. An important limit is where we take N to infinity so $\langle k\rangle \to 0$.

We will then assume that at each time step one edge is rewired [39]. Continuous time evolution is considered in Sec. VI A. At each time step [40] we first make two choices and only then do we change the network.

First an individual is chosen in some stochastic manner. This individual is attached by one edge to an artifact, the departure artifact. It is the artifact end of this edge which is to be changed. Thus we are effectively removing an edge from the departure artifact chosen with probability [41] Π_R. The edge chosen is going to be rewired and attached to another artifact vertex, the arrival artifact, picked with probability Π_A. Thus the master equation for the degree distribution in the mean-field approximation is

$$\begin{aligned} n(k,t+1) - n(k,t) = {} & n(k+1,t)\Pi_R(k+1,t)[1-\Pi_A(k+1,t)] \\ & - n(k,t)\Pi_R(k,t)[1-\Pi_A(k,t)] \\ & - n(k,t)\Pi_A(k,t)[1-\Pi_R(k,t)] \\ & + n(k-1,t)\Pi_A(k-1,t) \\ & \times[1-\Pi_R(k-1,t)] \quad (E \geq k \geq 0). \end{aligned} \tag{1}$$

For notational simplicity we choose to set $n(k)=\Pi_R(k)=\Pi_A(k)=0$ for the unphysical values $k=-1$ and $k=(E+1)$. In this way the equation gives the correct behavior at the physical boundary values of $k=0$ and $k=E$.

Note that there is a chance $(\Pi_R\Pi_A)$ that we will choose the same artifact vertex for both attachment and removal. As this produces no change in the network we must ensure that such events do not contribute to changes in the degree distribution. This is the role of the factors of $(1-\Pi)$. Such terms are not normally found in the master equations for network rewiring [3,5–9,11]. It is *crucial* that we do this otherwise we will not have the correct behavior at the boundaries $k=0$ and $k=E$.

Such $(1-\Pi)$ corrections will often be negligible especially for large E systems where the probabilities $\Pi(k)$ for any individual value of degree k may be tiny [42]. However, there are important configurations in this model and in related models where even for large systems in equilibrium $\Pi(k)$ are not small for some values of k. This will be discussed in Sec. VI A after we have obtained the explicit solution.

The master equation (1) is a mean-field approximation for the evolution through our stochastic dynamics of the average value of the function $n(k)$. The errors come if

$$\langle n(k,t)f(k,t)\rangle - \langle n(k,t)\rangle\langle f(k,t)\rangle \neq 0, \tag{2}$$

where f are various combinations of Π_R and Π_A. For instance, if we have a model with attachment or removal probabilities of the form (k^β/z_β) then the problem lies with the normalization as in general

$$\left\langle n(k,t)\frac{k^\beta}{z_\beta(t)}\right\rangle \neq k^\beta \frac{\langle n(k,t)\rangle}{\langle z_\beta(t)\rangle}. \tag{3}$$

In many practical cases the fluctuations are small and the corrections to the mean-field results are often found to be small. For this reason the equations can be a good approximation even if the number of vertices or edges fluctuate provided their average values are constant and the variations are small.

However, there are two special cases where equality holds in Eq. (3) implying that the mean-field approximation is exact, namely when $\beta=0$ or 1. Only in these cases are the normalizations of probabilities constants of the motion, N and E, respectively. The most general choice for Π_R and Π_A satisfying these criteria is therefore

$$\Pi_R = \frac{k}{E}, \quad \Pi_A = p_r\frac{1}{N} + p_p\frac{k}{E}, \quad p_p + p_r = 1 \quad (E \geq k \geq 0). \tag{4}$$

This form for Π_A means that an edge can be reattached in two ways. With probability p_p, *preferential attachment* is used and the artifacts are chosen with a likelihood proportional to their degree. Alternatively with probability p_r a random [43] artifact is chosen. Choosing a random edge for rewiring corresponds to the use of "preferential removal" alone.

There are other good reasons for choosing these forms for the probability apart from the fact the master equation is then exact. Mathematically, these simple forms enable us to find a complete nonequilibrium solution. In terms of practical applications, one may understand these special forms as emerging naturally from a random walk process [36,44]. We will also note the scaling properties of their solutions in Sec. VII. We will limit our analysis to the case (4) which means we will present exact results for the ensemble average of various quantities at any time and for any values of our parameters.

III. THE GENERATING FUNCTION

A useful way to investigate the degree distribution $n(k,t)$ is to encode it with a generating function $G(z,t)$,

$$G(z,t) \equiv \sum_{k=0}^{E} z^k n(k,t). \tag{5}$$

Below we will exploit the fact that G is always a polynomial in z of order no greater than E. The mean-field equations (1) can then be rewritten as a differential equation for the generating function,

$$\frac{b(1+a-c)}{(1-z)}[G(z,t+1)-G(z,t)] = z(1-z)G''(z,t)+[c-(a+b+1)z]G'(z,t)-abG(z,t), \tag{6}$$

where the differentials G'' and G' are with double and single derivatives with respect to z. The constants a, b, and c are given by

$$a=\frac{p_r}{p_p}\langle k\rangle, \quad b=-E, \quad c=1+\frac{p_r}{p_p}\langle k\rangle-\frac{E}{p_p}. \tag{7}$$

The equation for $n(k,t)$ is linear—it is completely equivalent to a Markov process in an $E+1$-dimensional space in which the vector $[n(0,t),n(1,t),\ldots,n(E,t)]$ lives [38]. Therefore we can define $E+1$ eigenvectors $\omega^{(m)}(k)$ associated with an eigenvalue λ_m ($m=0,1,2,\ldots,E$), which we order such that $\lambda_m \geq \lambda_{m+1}$. Furthermore, the properties of the Markov process guarantee that $1 \geq |\lambda_m|$ with at least $\lambda_0=1$.

We can now break the generating function into $E+1$ components with the time dependence factorized,

$$G(z,t)=\sum_{m=0}^{E} c_m(\lambda_m)^t G^{(m)}(z), \quad G^{(m)}(z)\equiv\sum_{k=0}^{E} z^k\omega^{(m)}(k), \tag{8}$$

where the coefficients c_m depend on the initial conditions $n(k,t=0)$. Again the generating functions for the eigenvectors, $G^{(m)}(z)$, are polynomials of degree no larger than E. Substituting this form into Eq. (6) gives a time-independent differential equation for $G^{(m)}(z)$, the generating function of the mth eigenvector:

$$z(1-z)G^{(m)''}(z)+[c-(a+b+1)z]G^{(m)'}(z)-\left[ab-\frac{(\lambda_m-1)}{1-z}b(c-a-1)\right]G^{(m)}(z)=0. \tag{9}$$

This can be solved most easily by writing G as a polynomial in $(1-z)$. Having the correct form for the master equation and therefore the correct behavior at the boundaries ensures that this gives a finite order polynomial. These may be summarized in terms of the hypergeometric function $F={}_2F_1$ to be [45]

$$G^{(m)}(z)=(1-z)^m F(a+m,b+m;c;z) \tag{10}$$

$$=(1-z)^m\sum_{l=0}^{E-m}\frac{\Gamma(a+m+l)\Gamma(b+m+l)\Gamma(c)}{\Gamma(a+m)\Gamma(b+m)\Gamma(c+l)(l\,!\,)}z^l \tag{11}$$

with corresponding eigenvalues,

$$\lambda_m=1-m(m-1)\frac{p_p}{E^2}-m\frac{p_r}{E}, \quad 0\leq m\leq E. \tag{12}$$

An expression for the entries of the eigenvectors $\omega^{(m)}(k)$ may be derived from the coefficients of z^k in Eq. (11) which can be given in terms of the hypergeometric function ${}_3F_2$, though it is not very illuminating and merely assists in explicit evaluations:

$$\omega^{(m)}(k)=(-1)^m\frac{\Gamma(k+1)}{\Gamma(k+1-m)}\frac{\Gamma(c+k)}{\Gamma(c+k-m)}\frac{\Gamma(a)}{\Gamma(a+m)}\frac{\Gamma(b)}{\Gamma(b+m)} \times {}_3F_2(-m,a+k,b+k;k+1-m,k+c-m;1-z)|_{z=0}\omega^{(0)}(k), \tag{13}$$

where

$$\omega^{(0)}(k)=\frac{\Gamma(a+k)}{\Gamma(a)}\frac{\Gamma(b+k)}{\Gamma(b)}\frac{\Gamma(c)}{\Gamma(c+k)}. \tag{14}$$

In the special case of $p_r=1$, the degree distribution is that of the Watts and Strogatz model [1] (see Sec. VI below). The generating function then reduces to

$$G^{(m)}(z)=\frac{1}{(1-N^{-1})^{E-m}}(1-z)^m[(1-N^{-1})+N^{-1}z]^{E-m}. \tag{15}$$

More usefully we note for later use that the eigenvalues satisfy [46]

$$1=\lambda_0>\lambda_1>\cdots\lambda_m>\lambda_{m+1}>\cdots\lambda_E=\frac{p_p}{E}>0 \quad (0<p_r\leq 1), \tag{16}$$

$$\lambda_1=1-\frac{p_r}{E}, \quad \lambda_2=1-\frac{2p_r}{E}-\frac{2p_p}{E^2}. \tag{17}$$

The first consequence of these solutions is that the system evolves to a unique equilibrium solution given by [37]

$$G(z)\equiv\lim_{t\to\infty}G(z,t)=c_0F(a,b;c;z). \tag{18}$$

The time scale for the decay of each of the eigenfunctions is given by

$$\tau_m=-1/\ln(\lambda_m). \tag{19}$$

IV. THE DEGREE DISTRIBUTION

The degree distribution $n(k,t)$ at any time is given as the coefficients of z^k in the expression for the generating function $G(z,t)$ of Eq. (8) and this in turn depends on the initial conditions. The equilibrium degree distribution derived from $G(z)$ of Eq. (18) which from Eq. (8) is based only on the zeroth eigenfunction $\omega^{(0)}$ [the $m=0$ case of Eq. (11)]. In particular the $k=0$ case shows that $c_0=n(0)=\lim_{t\to\infty}n(k=0,t)$ and so we have

$$n(k) := \lim_{t\to\infty} n(k,t) = \frac{1}{k!}\left.\frac{d^k G(z)}{dz^k}\right|_{z=0}$$
$$= \frac{n(0)}{\Gamma(k+1)}\frac{\Gamma(a+k)}{\Gamma(a)}\frac{\Gamma(b+k)}{\Gamma(b)}\frac{\Gamma(c)}{\Gamma(c+k)}. \quad (20)$$

The total number of artifacts is given simply by the generating function at $z=1$ so

$$N = c_0 G(z=1) = n(0)F(a,b;c;1). \quad (21)$$

This gives us the equilibrium artifact degree probability distribution function $p(k)=n(k)/N$ as

$$p(k) = A\frac{\Gamma\left(k+\frac{p_r}{p_p}\langle k\rangle\right)}{\Gamma(k+1)}\frac{\Gamma\left(\frac{E}{p_p}-\frac{p_r}{p_p}\langle k\rangle - k\right)}{\Gamma(E+1-k)}, \quad (22)$$

$$A := \frac{\Gamma\left(\frac{p_r}{p_p}E\right)\Gamma(E+1)}{\Gamma\left(\frac{p_r}{p_p}(E-\langle k\rangle)\right)\Gamma\left(\frac{p_r}{p_p}\langle k\rangle\right)\Gamma\left(\frac{E}{p_p}\right)}, \quad (23)$$

where we have chosen to write the expression in terms of Γ functions of positive arguments and in terms of the original parameters. Two useful values are the degree probability distribution for zero degree and maximum degree $k=E$. The former provides a measure of the number of unused artifacts and thus another measure of the uniformity of the system and the latter will be discussed in detail below. These satisfy simple formulas

$$p(0) = \frac{\Gamma\left(\frac{p_r}{p_p}E\right)}{\Gamma\left(\frac{E}{p_p}\right)}\frac{\Gamma\left(\frac{E}{p_p}-\frac{p_r}{p_p}\langle k\rangle\right)}{\Gamma\left(\frac{p_r}{p_p}E-\frac{p_r}{p_p}\langle k\rangle\right)}, \quad (24)$$

$$p(E) = \frac{\Gamma\left(\frac{p_r}{p_p}E\right)}{\Gamma\left(\frac{E}{p_p}\right)}\frac{\Gamma\left(E+\frac{p_r}{p_p}\langle k\rangle\right)}{\Gamma\left(\frac{p_r}{p_p}\langle k\rangle\right)}. \quad (25)$$

The results for $p(0,t)$ are plotted against exemplary data in Fig. 2.

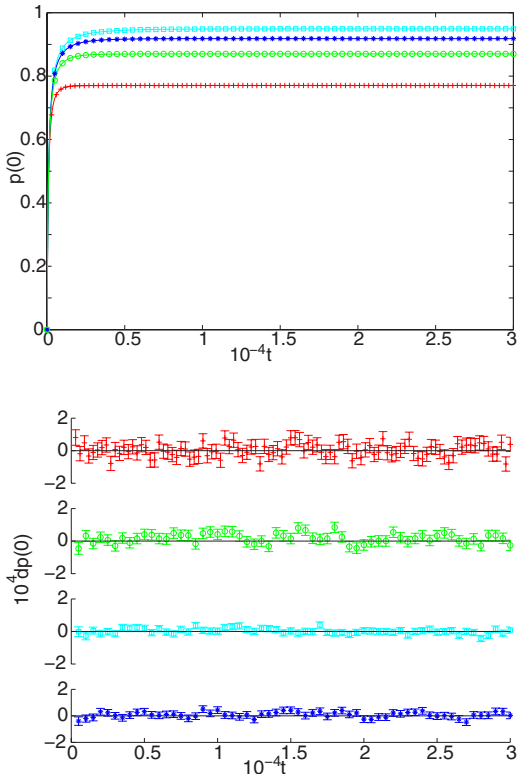

FIG. 2. (Color online) Plots of $p(0)$ and the fractional difference between the simulation and mean-field results ($dp(0)=[p_{\text{expt}}(0)/p_{\text{theor}}(0)]-1$) against the number of rewirings t; for $N=E=100$ and $p_r=0.1$ (crosses), $p_r=0.04$ (circles), $p_r=0.02$ (stars), and $p_r=0.01$ (squares). Simulations started with $n(k=1)=E$ and zero otherwise. Averaged over 10^6 runs. The solid lines are the results from the mean-field calculations.

A. Large degree equilibrium behavior

The solution for $p(k)$ has two significant parts. The first k dependent ratio of gamma functions in Eq. (22) for $k\gg 1$ and $p_r\approx 0$ behaves as

$$R_1 = \frac{\Gamma\left(k+\frac{p_r}{p_p}\langle k\rangle\right)}{\Gamma(k+1)} \propto k^{-\gamma}\left[1+O\left(k^{-1},\frac{p_r\langle k\rangle}{p_p k}\right)\right],$$
$$\gamma = 1-\frac{p_r}{p_p}\langle k\rangle \le 1. \quad (26)$$

For $p_r=0$ or $\langle k\rangle=0$ (which includes when $N\to\infty$) this term gives us an exact inverse k power law for all degrees k from this term. Another special case corresponds to an attachment probability of $\Pi_A \propto (k+1)$ which is often found in the literature, for instance, [7,10,11]. This ratio R_1 is then exactly one for all k so $\gamma=0$. In general the power is usually close but always less than one.

However, the $(1-\Pi_A)$ and $(1-\Pi_R)$ terms in Eq. (1) have led to the second k-dependent ratio of gamma functions in Eq. (22). If $E\gg k$ this gives an exponential cutoff

$$R_2 = \frac{\Gamma\left(\frac{E}{p_p}-\frac{p_r}{p_p}\langle k\rangle - k\right)}{\Gamma(E+1-k)} \propto \exp\{-\zeta k\}\left[1+O\left(\frac{k}{E},\frac{\langle k\rangle}{E}\right)\right], \quad (27)$$

$$\zeta = -\ln(p_p) \quad (28)$$

$$\approx p_r \quad \text{if } p_r \ll 1, \quad \langle k\rangle \ll E. \quad (29)$$

Within these approximations, this may be expressed in an equivalent manner which is sometimes seen in the literature (e.g., [23,24,28])

$$R_2 = \frac{\Gamma\left(\frac{E}{p_p} - \frac{p_r}{p_p}\langle k\rangle - k\right)}{\Gamma(E+1-k)} \propto \left(1-\frac{k}{E}\right)^{E\bar{\zeta}}\left[1+O\left(\frac{k}{E}\right)\right], \tag{30}$$

$$\bar{\zeta} = \frac{p_r}{p_p}\left(1-\frac{1}{N}\right) - \frac{1}{E} \approx p_r. \tag{31}$$

While not strictly valid at $k \approx E$ this second form indicates that there is a change of behavior for large degree if $\bar{\zeta} < 0$. In such a case the numerator of this second k-dependent ratio of gamma functions becomes very large for $k=E$ and we see directly that this happens if $p_r \ll p_\sharp$, where $R_2 = 1$ ($\bar{\zeta}=0$) at $p_\sharp$:

$$p_\sharp = \frac{1}{E+1-\langle k\rangle} \approx \frac{1}{E}[1+O(\langle k\rangle E^{-1})]. \tag{32}$$

At $p_r = p_\sharp$ we are closest to a pure power law with a power $\gamma = \gamma_\sharp = 1-(2N)^{-1}$. For the special case where $N\to\infty$ so $\langle k\rangle \to 0$ we get a perfect inverse power law at $p_r = (1+E)^{-1}$.

As p_r drops below this critical value, a spike emerges at $k=E$ from this second k-dependent ratio R_2 which comes to dominate the degree distribution at $p_r \to 0$. The point where the distribution has become flat at the upper boundary, so $n(E) = n(E-1)$, defines an alternative critical random attachment probability p_* at

$$p_* = \frac{E-1}{E^2 + E(1-\langle k\rangle) - 1 - \langle k\rangle}, \tag{33}$$

$$Ep_* \approx 1 + \frac{(\langle k\rangle - 2)}{E}. \tag{34}$$

Either way when $p_r \lesssim 1/E$ the degree distribution will show a spike at $k=E$.

Overall we see two distinct types of distribution. For large random attachment rates, $Ep_r \gtrsim 1$, we get a simple inverse power with an exponential cutoff

$$n(k) \propto (k)^{-\gamma}\exp\{-\zeta k\}, \quad p_r \gtrsim \frac{1}{E}. \tag{35}$$

This behavior is often noted in the literature [5–7,17,18,23,24,27] and the formulas given there for the power γ and cutoff ζ or $\bar{\zeta}$ are consistent with the exact formulas given here given the various approximations used elsewhere. Note that in any one practical example it will be impossible to distinguish the power γ derived from the data from a value of one. This is because to have a reasonable section of power law behavior we require $1 \ll \zeta$ but this implies that p_r is small and so $(\gamma-1) \ll \langle k\rangle$. The power drifts away from one as we raise the random attachment rate p_r towards one but only at the expense of the exponential regime starting at a lower and lower degree. Only when the power is very close to one can we get enough of a power law to be significant.

However, as p_r is lowered towards zero we get a change of behavior in the exponential tail around $p_r E \approx 1$. First we find that the exponential cutoff ζ^{-1} moves to larger and larger values, eventually becoming bigger than E. For p_r slightly below $p_\sharp$, that is for $p_r > p_* \approx E^{-1}$, the tail starts to rise. For $p_r E \ll 1$, i.e., if there has been no random artifact chosen after most edges have been rewired once, then we will almost certainly find one artifact linked to most of the individuals, $n(E) \approx 1$.

This behavior for $Ep_r \ll 1$ has been noted in some of the literature where it is known as *condensation* [12,14–18] or, in the older population genetics literature, it is called *fixation*. It mirrors similar behavior known for growing networks when nonlinear attachment probabilities or vertex fitness are used, for example, see [33,47].

B. Limiting values of p_r in equilibrium

The $p_r = 0$ limit offers some simplifications as well as being the only value in the condensation phase. The condensation is clear from the expression for $p(k)$ of Eq. (22) as the denominator is infinite if $(p_r/p_p)E(1-N^{-1}) = 0$, i.e., either we have the trivial example of one artifact $N=1$ or we are in the pure preferential attachment limit $p_p = 1, p_r = 0$. For the latter $p(k)$ is therefore zero for all values of k except $k=0$ or $k=E$ where the infinity is canceled by the same term in the numerator. For instance, we find that [48] for small p_r the equilibrium distribution has the form

$$p(0) \approx \left(1-\frac{1}{N}\right)\{1 - p_r\langle k\rangle[\psi(E) - \psi(1)]\} + O[(p_r)^2], \tag{36}$$

$$p(k) \approx p_r \frac{\langle k\rangle(E-\langle k\rangle)}{k(E-k)} + O(p_r^2), \quad 0 < k < E, \tag{37}$$

$$p(E) \approx \frac{1}{N}\{1 - p_r(E-\langle k\rangle)[\psi(E) - \psi(1)]\} + O[(p_r)^2], \tag{38}$$

so only at $p_r = 0$ do we get condensation for any E. This represents a true phase transition in the large system ($E \to \infty$, thermodynamic) limit between the gamma distribution (35) for $p_r > 0$ and the condensation $p(k) = \delta_{k,E}$ at $p_r = 0$.

At the other extreme, we have the limit of pure random artifact selection $p_r = 1$. In this limit the model captures exactly the degree distribution of the original Watts and Strogatz model [1]. In this case for any E and $\langle k\rangle$ the solution for $p(k)$ [Eq. (22)] reduces to a binomial distribution with a probability $(1/N)$ of any one edge connecting to a given artifact vertex, i.e., we have the expected Erdős-Réyni random graph in the long time limit.

C. Time dependence of the degree distribution

So far we have looked at the equilibrium behavior but we have a complete solution for the degree distribution for all times and any value of the parameters through our eigenfunctions (13) and eigenvalues (12). Alternatively for small values of E it may be more convenient to cast this as a matrix

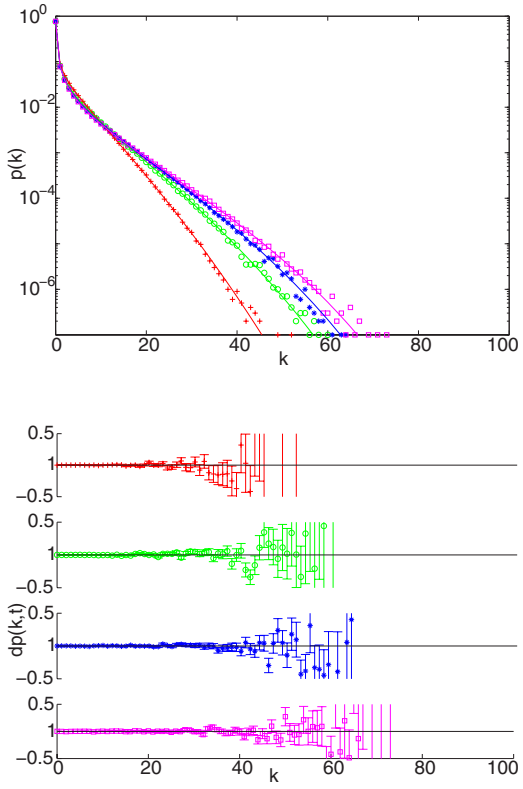

FIG. 3. (Color online) Plots of $p(k)$ and the fractional deviation $[dp=p_{\text{expt}}(k,t)/p_{\text{theor}}(k,t)-1]$ between the simulation (data points) and exact mean-field results (lines); for $E=N=100$ and $p_r=0.1$ after evolving for $t\approx\tau_2$ (crosses), $t\approx 2\tau_2$ (circles), $t\approx 3\tau_2$ (stars), and to equilibrium (squares). The solid lines are the relevant mean-field results plotted for the same times. Started with $n(k=1)=E$ and zero otherwise and simulation results averaged over 10^5 runs.

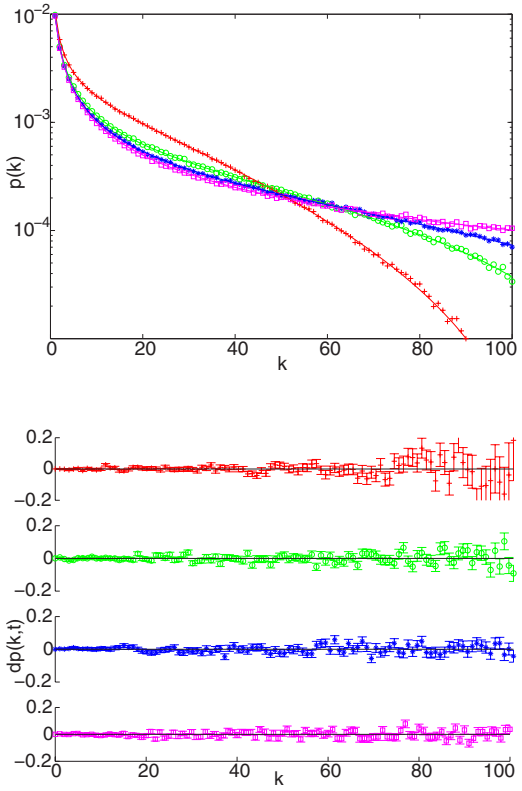

FIG. 4. (Color online) Plots of $p(k)$ and the fractional deviation $[dp=p_{\text{expt}}(k,t)/p_{\text{theor}}(k,t)-1]$ between the simulation (data points) and exact mean-field results (lines); for $E=N=100$ and $p_r=0.01$ after evolving for $t\approx\tau_2$ (crosses), $t\approx 2\tau_2$ (circles), $t\approx 3\tau_2$ (stars), and to equilibrium (squares). The solid lines are the relevant mean-field results plotted for the same times. Started with $n(k=1)=E$ and zero otherwise and simulation results averaged over 10^5 runs.

problem [38]. We have used the latter to predict the degree distribution for any time for a range of p_r values on either side of and approximately equal to the critical value p_* in Figs. 3–5. These (and other figures below) show that the degree distribution evolves on time scales τ_2 set by eigenvalue number two whatever p_r we use (why it is not τ_1 is explained below). Again the exact mean-field results fit the averaged values from a simulation extremely well.

V. THE MOMENTS OF THE DEGREE DISTRIBUTION

The properties of the hypergeometric function mean it is easy to calculate derivatives of the generating function at $z=1$ at *any* time as we have

$$g_n^{(m)} := \left.\frac{d^n G^{(m)}(z)}{dz^n}\right|_{z=1} \tag{39}$$

$$=(-1)^m g_0^{(0)} \frac{\Gamma(n+1)}{\Gamma(n+1-m)}\frac{\Gamma(a+n)}{\Gamma(a+m)}\frac{\Gamma(b+n)}{\Gamma(b+m)} \times \frac{\Gamma(c-n-m-a-b)}{\Gamma(c-a-b)}\frac{\Gamma(c-a)}{\Gamma(c-a-m)}\frac{\Gamma(c-b)}{\Gamma(c-b-m)}$$

$$(m \le n) \tag{40}$$

with $g_n^{(m)}=0$ if $m>n$. This then suggests that rather than work in terms of the higher moments $\langle k^n\rangle$, we use the probabilities F_n where [49]

$$F_n(t) := \frac{\Gamma(E+1-n)}{\Gamma(E+1)}\left.\frac{d^n G(z,t)}{dz^n}\right|_{z=1} = \sum_{k=0}^{E} \frac{k}{E}\frac{(k-1)}{(E-1)}\cdots\frac{(k-n+1)}{(E-n+1)} n(k,t). \tag{41}$$

The function F_n is the probability that if we choose n distinct edges, they will all share the same artifact. The rth moment $\langle k^r\rangle$ can be calculated if given all the F_n for $n\le r$. The F_n achieve their largest value only when we have a condensation, $p(k)=(N-1)\delta_{k,0}+\delta_{k,E}$, where $F_n=1$ for all $n\ge 2$. That is we have a perfectly homogeneous population (all the individuals are connected to the same artifact). The lowest possible value of F_n depends on the other parameters. If we have $E\le N$ then when all artifacts have at most one edge attached then $F_n=0$ for all n, as we can see in Fig. 6 at the initial time. The evolution causes a drift towards a more heterogeneous distribution. The same figure also shows how the exact mean-field results match results from simulations extremely well. Mathematically it is clear from the result (11) that the

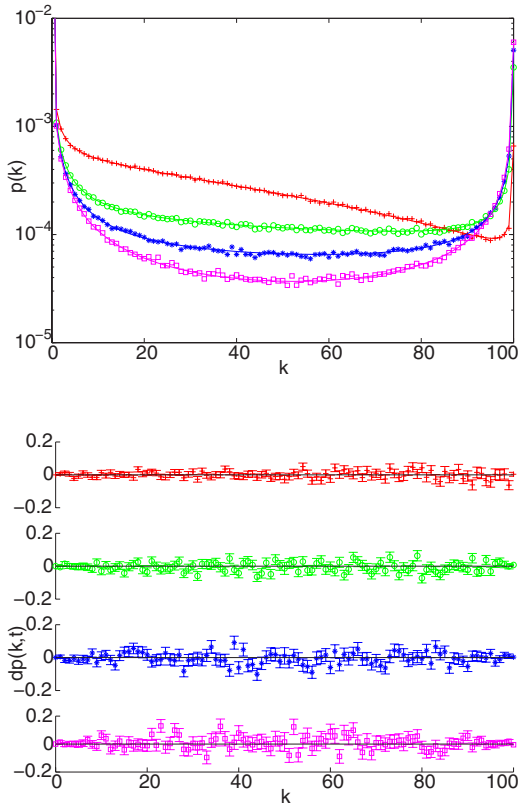

FIG. 5. (Color online) Plots of $p(k)$ and the fractional deviation $[dp=p_{\text{expt}}(k,t)/p_{\text{theor}}(k,t)-1]$ between the simulation (data points) and exact mean-field results (lines); for $E=N=100$ and $p_r=0.001$ after evolving for $t\approx\tau_2$ (crosses), $t\approx 2\tau_2$ (circles), $t\approx 3\tau_2$ (stars), and to equilibrium (squares). The solid lines are the relevant mean-field results plotted for the same times. Started with $n(k=1)=E$ and zero otherwise and simulation results averaged over 10^5 runs.

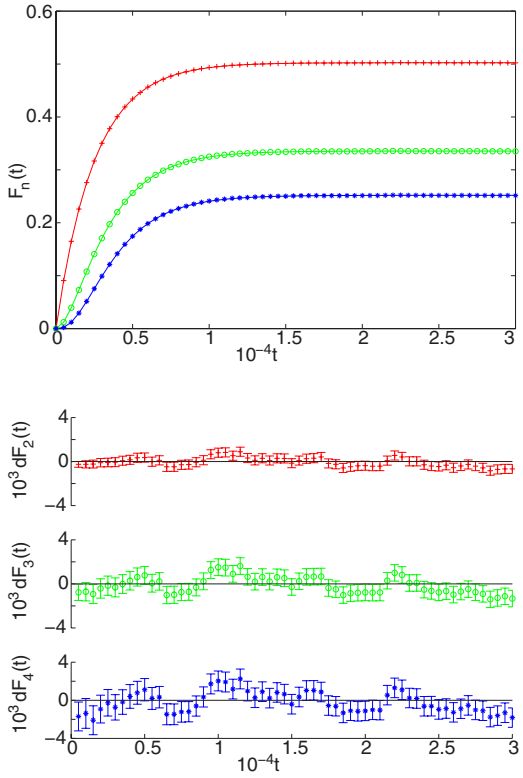

FIG. 6. (Color online) Plots of various $F_n(t)$ for numerical simulations (points) with their exact mean-field predictions (lines) against the number of rewirings t. From top to bottom we have $F_2(t)$ (crosses), $F_3(t)$ (circles), and $F_4(t)$ (stars). The second plot shows the fractional difference between numerical experiments and theoretical results $dF_n=(F_{n,\text{expt}}/F_{n,\text{theor}})-1$; for $E=N=100$, $p_r=0.01$ and data points are the average of 10^5 runs of a simulation.

F_n only has contributions from the first $n+1$ eigenfunctions, i.e., from $G^{(m)}$ for $m\leq n$.

In equilibrium only eigenfunction zero contributes and we have a simple result

$$\lim_{t\to\infty} F_n(t) := F_n = N\frac{\Gamma\left(\frac{p_r}{p_p}\langle k\rangle + n\right)\Gamma\left(\frac{p_r}{p_p}E\right)}{\Gamma\left(\frac{p_r}{p_p}\langle k\rangle\right)\Gamma\left(\frac{p_r}{p_p}E + n\right)}. \quad (42)$$

A. Normalization N

The zeroth moment sets the overall normalization of the degree distribution $n(k,t)$. This is nothing but the total number of artifact nodes N and for any time t we find it is equal to

$$N = G(z=1,t) = \sum_{m=0}^{E} c_m(\lambda_m)^t g_0^{(m)} = c_0 F(a,b;c;1). \quad (43)$$

This result is time independent because it comes only from the zeroth eigenvector, the only time independent part of the solution. Thus our solution is consistent with a key property in this model, namely the constant number of artifacts N. This then fixes the amplitude of the zeroth eigenfunction in Eq. (8) to be

$$c_0 = \frac{N}{g_0^{(0)}}. \quad (44)$$

B. Average degree

The first derivative of the generating function gives the number of edges

$$E = \left.\frac{d}{dz}G(z,t)\right|_{z=1} \quad (45)$$

$$= \sum_{m=0}^{E} c_m(\lambda_m)^t g_1^{(m)} = \frac{c_0}{N}g_1^{(0)} + \frac{c_1}{N}(\lambda_1)^t g_1^{(1)}. \quad (46)$$

Only eigenfunctions zero and one contribute but the latter leads to time dependence. On the other hand we also have a fixed number of edges in this model as it is one of our input parameters. The only solution is therefore $c_1=0$. Thus for any physical problem there is no contribution from eigenfunction number one.

This equation then appears to overconstrain our solution as c_0 is already known from the normalization (44) and all other quantities are fixed. However, we find that using standard properties of hypergeometric functions and the normalization from Eq. (43) that the solution already satisfies Eq. (45) and again everything is consistent.

C. Homogeneity measures F_n and initial conditions

The next derivative of the generating function contains the second moment but it is preferable to work with our related function F_2—the probability that two distinct edges chosen at random are connected to the same artifact. Similar measures of the homogeneity of the artifact choices have been used before such as $F=\langle(k^2/E^2)\rangle$ but this is easily calculated from our F_2 measure. We find that

$$F_2(t) := \sum_{k=0}^{E} \frac{k(k-1)}{E(E-1)} n(k,t) \tag{47}$$

$$= \frac{1}{E(E-1)}[c_0 g_2^{(0)} + c_2(\lambda_2)^t g_2^{(2)}]. \tag{48}$$

Now there is time dependence but only coming from eigenfunction number two. This function is readily evaluated using Eq. (40), the coefficient c_2 fixed upon specification of the initial conditions. This formula fits the results extremely well as Fig. 7 shows.

One of the advantages of the F_n measures is that they provide a systematic and practical way of fixing the amplitudes of each eigenfunction, the c_m coefficients of Eq. (8), from the initial conditions. From the definition (41) we can express F_n in terms of the nth derivatives of the generating functions associated with the mth eigenfunction evaluated at $z=1$, i.e., $g_n^{(m)}$ of Eq. (39).

$$\frac{\Gamma(E+1-n)}{\Gamma(E+1)} \sum_{m=0}^{n} c_m g_n^{(m)} = F_n(t=0). \tag{49}$$

However, only the first n eigenfunctions contribute so we can use an iterative scheme to find the first few coefficients quickly. These are sufficient to provide an excellent approximation for the degree distribution for most times.

For example, consider the case of uniform initial conditions, such that $E \leq N$ and each artifact is connected to at most one edge, then we have that $F_n=0$ for $n \geq 2$. This corresponds to the choice of initial conditions used in obtaining the numerical results in Figs. 2–5. So for these initial conditions the following condition holds:

$$\sum_{m=0}^{n} c_m g_n^{(m)} = 0, \quad n \geq 2. \tag{50}$$

We have already seen that the N parameter fixes c_0 in Eq. (44) while the first moment or equivalently E gives $c_1=0$. So starting with $n=2$ we have

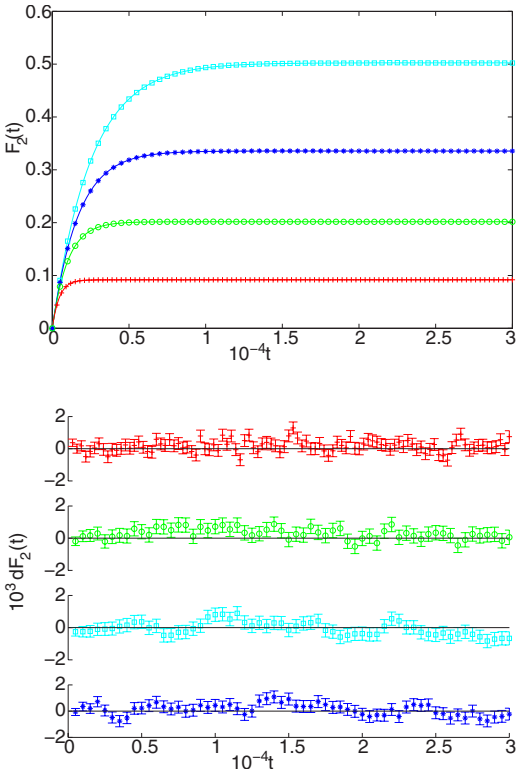

FIG. 7. (Color online) Plots of the homogeneity factor $F_2(t)$ and the fractional difference between the simulation (data points) and exact mean-field results (lines) against the number of rewirings t; for $N=E=100$ and different p_r. From bottom to top: $p_r=0.1$ (crosses), $p_r=0.04$ (circles), $p_r=0.02$ (stars), and $p_r=0.01$ (squares). The second plot shows the fractional difference between numerical experiments and theoretical results $dF_2=(F_{2,\text{expt}}/F_{2,\text{theor}})-1$. The initial configuration is $n(k=1)=E$ and zero otherwise. Simulation data is averaged over 10^4 runs. The results are in good agreement with the analytic result equation (52).

$$c_2 = -c_0 \frac{g_2^{(0)}}{g_2^{(2)}}. \tag{51}$$

The exact time dependence of the second homogeneity function is

$$F_2(t) = (1-\lambda_2^t)F_2(\infty)$$
$$= (1-\lambda_2^t)\frac{p_p + p_r\langle k\rangle}{p_p + p_r E}. \tag{52}$$

Comparisons to numerical results are plotted in Fig. 7.

Another particularly convenient choice of initial conditions is to attach each individual vertex to the same artifact vertex so that $n(k=E)=1$, $n(k=0)=N-1$, and zero otherwise. Now $F_n(0)=1$ and the condition (49) becomes

$$\sum_{m=0}^{n} c_m g_n^{(m)} = \frac{\Gamma(E+1)}{\Gamma(E+1-n)}. \tag{53}$$

Note, we have put no restriction on the total number of individual vertices, E. For the simplest case $n=2$ we are led to

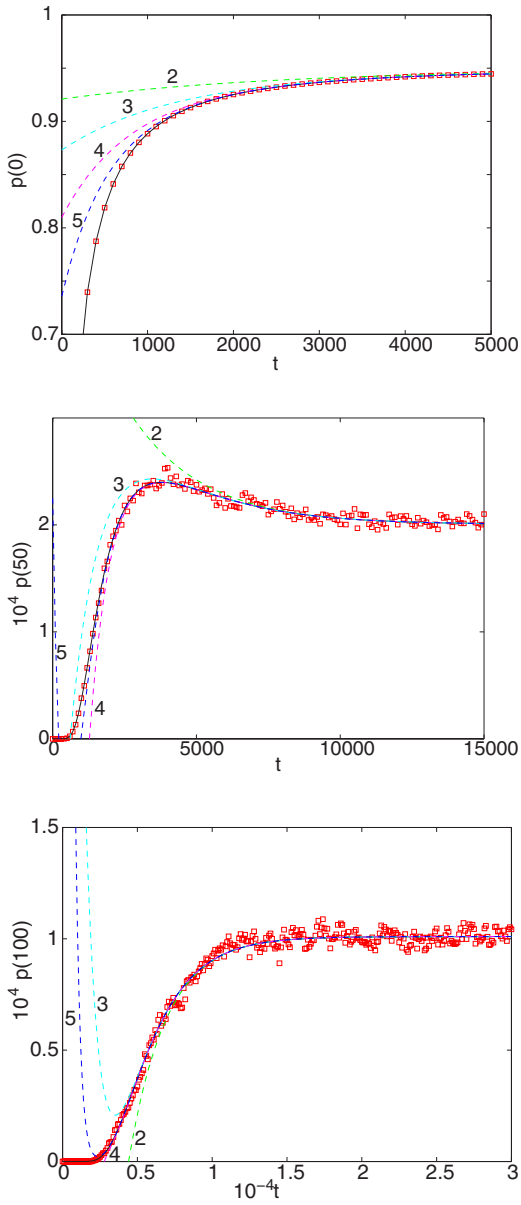

FIG. 8. (Color online) Plots of the evolution of $p(0)$, $p(50)$, and $p(100)$ against the number of rewirings t for $E=N=100$, $p_r=0.01$ compared with the relevant mean-field results. The solid lines represent the exact mean-field solution, while the numbered dashed lines indicate the successive improvements obtained using contributions from λ_2 (2) up to λ_5 (5). Simulations started with $n(k=1)=E$ and zero otherwise. Averaged over 10^5 runs.

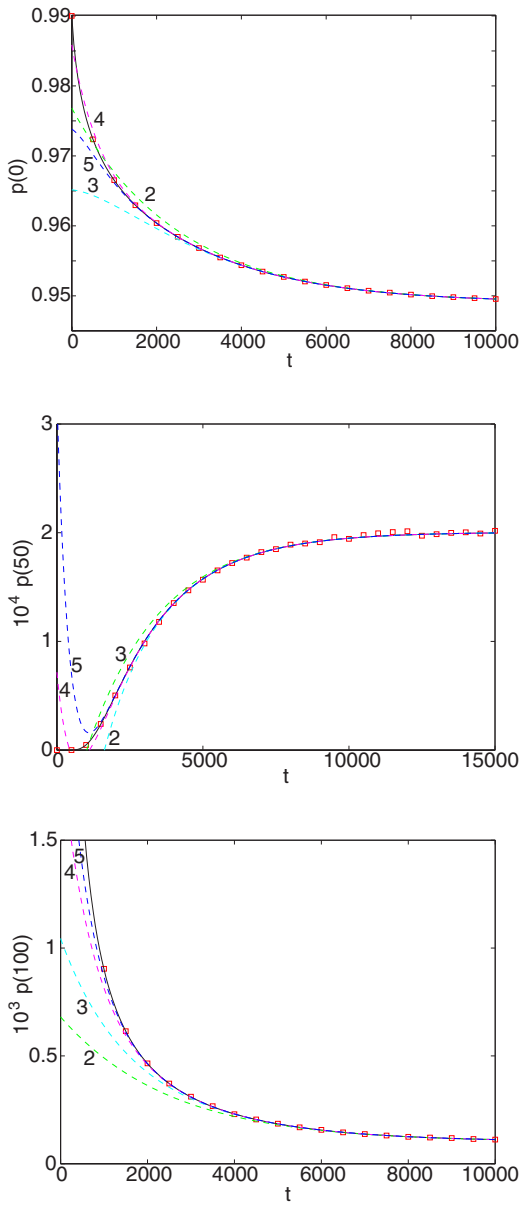

FIG. 9. (Color online) Plots of the evolution of $p(0)$, $p(50)$, and $p(100)$ against the number of rewirings t for $E=N=100$, $p_r=0.01$ compared with the relevant mean-field results. The solid lines represent the exact mean-field solution, while the numbered dashed lines indicate the successive improvements obtained using contributions from λ_2 (2) up to λ_5 (5). Simulations started with the alternate initial condition $n(k=E)=1$. Averaged over 10^6 runs.

another simple formula,

$$F_2(t) = (1-\lambda_2^t)\left(\frac{p_p + p_r\langle k\rangle}{p_p + p_r E} - 1\right) + 1. \tag{54}$$

While the exact degree distribution requires knowledge of all the eigenfunctions, the low n eigenfunctions still provide a suitable approximation for most times. Figures 8 and 9 illustrate this, showing the contributions to the degree distribution from successive eigenvectors for the two initial conditions discussed above.

VI. DISCUSSION OF OTHER MODELS

The bipartite network of Fig. 1 represents relationships at the core of many models in the literature, some of which are not usually expressed in terms of networks. While the models considered elsewhere often have additional elements compared with our simple model of Sec. II, those models often contain special cases where the degree distributions for any time will be given by our exact result. The aim of this section is to indicate the relationship between our model and those found elsewhere. Only some of these connections have been made before and then only in some of the literature. We

will start by considering some generalizations of our simple model as this will then help us to make comparisons with previous work.

A. Generalizations of our bipartite model

Many related models work in continuous time so that the number of rewiring events which have occurred corresponds to our discrete time variable. However, it is easy to recast our simple model as a continuous time process so that $n(k,t+1)-n(k,t)$ on the left-hand side of our master equation (1) becomes $dn(k,t)/dt$ with the Π_R and Π_A being interpreted as rates. This case is just as easy to solve as we replace the form used before for our degree distribution and generating function (5) by

$$n(k,t) = \sum_{m=0}^{E} c_m \omega^{(m)}(k) \exp\{-\bar{\lambda}_m t\}, \quad \bar{\lambda}_m = 1 - \lambda_m. \quad (55)$$

The eigenfunctions $\omega^{(m)}(k)$ and the associated generating functions $G^{(m)}$ are exactly as before, the new eigenvalues $\bar{\lambda}_m$ have a simple relationship to our original λ_m and the form of the time dependence is altered. Thus our exact solutions may be applied to discrete or continuous time.

Another obvious generalization of our model is to alter the form of the attachment and removal probabilities Π_R and Π_A [Eq. (4)]. Suppose

$$\Pi_R(k) = q_p \frac{k}{E} + q_a \frac{(1-\delta_{k,0})}{N_a(t)}, \quad (56)$$

$$\Pi_A(k) = p_p \frac{k}{E} + p_a \frac{(1-\delta_{k,0})}{N_a(t)} + p_r \frac{1}{N}, \quad (57)$$

with $q_p+q_a=1$ and $p_p+p_a+p_r=1$. We have added an extra process to our model where with probability p_a (q_a) we can attach (remove) an edge from a random artifact chosen uniformly from those which have at least one edge. The number of such *active* artifacts, those where $k>0$, is denoted $N_a(t)$ and this is time-dependent. However, the master equation (1) will no longer be exact because N_a varies from configuration to configuration so averages of ratios of $k^m n(k)$ and N_a will not factorize into the ratio of their averages (2). The time dependence of $N_a(t)$ also makes the nonequilibrium solutions of the master equation hard to find though the equilibrium solution can be found as before [37]. For instance, the slope of the power law section in the noncondensed phase is now

$$\gamma = 1 - \left(\frac{p_r}{p_p} + \frac{p_a}{p_p} - \frac{q_a}{q_p} \right) \langle k \rangle \quad (58)$$

and it can now be greater than one. In terms of the condensed phase, this now occurs when $p_p > q_p$ which means that there is now a range of parameter values which lead to this phase for large networks.

Another obvious generalization is to have terms in Π_A or Π_R proportional to general powers of the degree (k^β/z_β) or powers of general functions $(a+bk)^\beta$. As noted in Sec. II this means that the master equation (1) is then only an approximation though in many cases it will be a good one.

An important aspect of our model is that we have events where an edge is rewired back to the same artifact so that the configuration does not change. We had to include the $(1-\Pi)$ factors to account for this correctly. If we wish we can exclude these events which correspond to choosing an attachment probability of the form

$$\Pi_A(d,a) = \left[\tilde{p}_r \frac{1}{(N-1)} + \tilde{p}_p \frac{k_a}{E-k_d} \right] (1-\delta_{d,a}), \quad \tilde{p}_p + \tilde{p}_r = 1, \quad (59)$$

where we are removing an edge from the artifact labeled d (the departure artifact) and adding it to an artifact labeled a (the arrival artifact). The $(1-\Pi)$ factors in the master equation (1) are now always one and can be dropped, giving the master equation the form often seen in the literature (e.g., in [3,5–9,11]). However, the preferential attachment term $\tilde{p}_p$ of the attachment probability Π_A now has a configuration dependent normalization. The mean-field master equation is now an approximation for all $\tilde{p}_p > 0$ and it is hard to solve it for arbitrary times. In many cases the fluctuations will be small and the mean field will be a good approximation. Further if the number of edges attached to any one artifact is small (tends to zero in the large E limit) then the difference between our model and one excluding $a=d$ events will be small [3]. Unfortunately, this will not be true in the interesting case where we have a condensation since for some artifact vertices k_a/E will be significant, finite even in the large E limit. We would then expect differences between processes based on Eqs. (4) and (59).

Ultimately we could make the attachment or removal rates depend on the individual nature of each vertex, e.g., make the probabilities p_r and p_p vary with artifact vertices. This could mimic "fitness" where some artifacts are intrinsically more likely to attract edges.

One realistic way that artifact fitness could emerge is through the addition of an artifact graph. That is we could add a second network which connects artifacts to artifacts and this could be used in choosing how the bipartite graph is rewired. For instance, suppose we have chosen the edge we are going to rewire so that we know the departure artifact. We could choose the arrival artifact by making a random walk on the artifact graph starting from the departure artifact [36,44]. In this way the artifacts with a high degree in the artifact graph would be preferred (even for a walk of one step) and a natural fitness assignment for artifacts has emerged. Alternatively, we could view this artifact graph as a way of encoding some distance metric on the artifact space. That is when choosing a random artifact, a p_r event, it may be that a small variation in the artifact, as defined by some metric, is more likely than a large one. Our simple model is equivalent to having a complete graph with tadpoles [50] for the artifact graph (the adjacency matrix is one for all entries) which we use for the random choice (p_r) events. The variation mentioned above, where reconnection to the same artifact is excluded, corresponds to a complete artifact graph with no tadpoles.

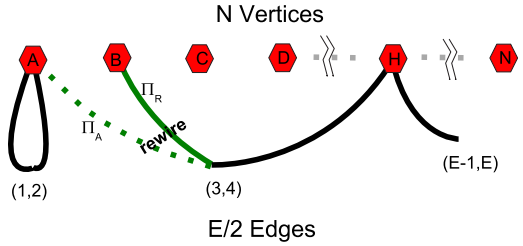

FIG. 10. (Color online) How the rewiring of the bipartite graph represents the rewiring of an undirected unipartite graph. In this example individual vertices numbers $(2i)$ and $(2i-1)$ are paired in the bipartite graph to give the edge labeled $(2i-1,2i)$ in the equivalent undirected graph. The rewiring of the undirected graph depicted in this figure is equivalent to that shown for the bipartite graph rewiring of Fig. 1. This is the projection used by Molloy and Reed [53].

At the moment, our preferential attachment process, p_p, has been put in by hand. However, this can emerge naturally if we add an individual graph, one which just connects the individual vertices. Suppose we have chosen the individual whose edge is to be rewired. We now make a random walk on the individual graph and arrive at an individual vertex which is connected to what is now taken to be the arrival artifact for the rewiring process. Even a short walk of this type produces good approximations to preferential attachment processes [36,44,51,52]. The preferential attachment events in our simple model are equivalent to doing a random walk on an individual graph which is a complete graph with tadpoles.

B. Relationship to models in the literature

The rewiring of unipartite networks has been studied in its own right [1–7,10,11] but all of these examples contain, in some sense, our bipartite graph. A projection of our bipartite graph gives a unipartite graph, made from just the artifact vertices. One way to achieve this example is to pair the individual vertices [say individuals numbered $(2i-1)$ with $(2i)$] and to consider the two edges of these individual vertices as the two ends (the stubs) of a single edge in the new undirected graph. Thus the process our simple model illustrated in Fig. 1 represents a rewiring process in some undirected graph as shown in Fig. 10. In this way, or by considering the problem directly, we see that the mean-field equations (1) are the same and we need only alter the normalizations in the probabilities (4).

Note that the degree distribution of the projected undirected graph at any one time is independent of how we pair off individual vertices in the bipartite graph. Thus the degree distributions of many different unipartite networks is represented by the same bipartite graph. Indeed this is the same projection used by Molloy and Reed to construct general random graphs, that is graphs of a given degree distribution but otherwise arbitrary [53].

There are several expressions for global properties of large generalized random graphs which depend on the ratio of the second and first moments through a parameter z [53–56]

$$z(t) := \frac{\langle k^2 \rangle}{\langle k \rangle} - 1 = (E-1)F_2(t). \tag{60}$$

Thus for large general random graphs being rewired using any mixture of random vertex and preferential attachment, we can give these global properties at *any* time. For instance, the mean intervertex distance ℓ scales as $(\ln(N)/\ln[z(t)+\text{const}])$ so we see from Eq. (52) that for large E we only avoid ℓ scaling as $\ln(N)$ if $p_r E \sim O(1)$.

Similarly a GCC (giant connected component) is present in this unipartite projection when $z>1$. We see that this will always appear if $\langle k \rangle > 1$ or, if $\langle k \rangle < 1$, it appears only if $p_r < (2-\langle k \rangle)^{-1}$. Suppose we start from the most disconnected example where $F_2(t=0)=0$ (so $\langle k \rangle \leq 1$). Using Eq. (52) we can find the time at which the GCC first appears. If $p_r E \sim O(1)$, which includes the condensate region, we find that the GCC appears at $t=E/2$. This is much quicker than the approach to the equilibrium configuration which happens on a time scale $\tau_2 \sim O(E^2)$. If p_r is raised from $O(E^{-1})$ towards the critical value for the existence of a GCC, $(2-\langle k \rangle)^{-1}$, the time at which the GCC appears increases, reaching infinity at the critical value of p_r.

A different example of this projection is when our initial bipartite graph has each artifact connected to m individuals $[n(k)=N\delta_{km}]$. The unipartite graph projection is then a randomized version of the graphs used by Watts and Strogatz [1]. From this initial condition and setting $p_r=1$ we therefore have the exact solution for the degree distribution at any time in the Watts and Strogatz model. The pairwise correlation of individual vertices is only required if we want to know about other aspects of the Watts and Strogatz networks, such as the network distance and clustering coefficients which were the focus of [1]. We can, however, calculate such quantities at any time in the randomized graph which provides a useful comparison.

It is straightforward to adapt this projection so that we get a directed graph. For instance, the direction of an edge in the projected unipartite graph could flow from the artifact connected to individual $(2i-1)$ to the artifact connected to individual $(2i)$. A simple modification of the master equation (1) is needed to keep track of the in- and out-degree if we choose to make these edges directional.

One can also think of other types of projection onto unipartite graphs. Suppose one fuses each individual vertex i with an artifact vertex which is not necessarily the artifact connected to that individual by the individual's edge in the bipartite graph. The individual-artifact edges of the bipartite graph now represent edges between the fused vertices of this projected unipartite graph. There is a natural direction associated to these unipartite edges coming from the individual-artifact direction of the bipartite graph, and this can be maintained or ignored as needed. A simple example of this projection is where the numbers of individual and artifact vertices are the same and we fuse each artifact vertex with one individual vertex. If we let the edges of the bipartite graph represent edges from the individual to an artifact in the unipartite graph, then the unipartite graph vertices have out-degree equal to one and this is one way of representing the

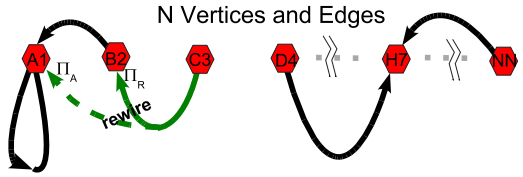

FIG. 11. (Color online) Another type of projection from our bipartite to a unipartite network. Each individual vertex is fused with one of the N artifact vertices to produce a unipartite graph with N vertices. The edges of the unipartite graph are naturally directional coming from the vertex associated with the old individual vertex of the bipartite graph and going to the old artifact vertex. In the simplest case we have the same number of artifacts E as individuals N and then we fuse artifact A with individual 1 to give a unipartite vertex labeled $A1$, etc. This produces a network of the type used in [5]. The figure shown here is this simple projection of the bipartite graph and rewiring event of Fig. 1.

degree distribution of the graphs of [5] and as illustrated in Fig. 11. Our master equation (1) is then the exact mean-field description for the in-degree in this case.

We will now turn to problems where there is no explicit reference to a network in the standard exposition but which can still be related to our model. In such cases there is an implicit graph in the problem which one may define to make contact with our realization, but this network may not be relevant in these other studies.

The work on cultural transmission [20–25] is usually developed without reference to any network. The names for our vertices come from this case. In this context individuals are deemed to be choosing some artifact of no particular value (pottery designs, pedigree dog breeds, or baby names, for example) by *copying* the choice of another individual—preferential attachment. Sometimes though one can expect *innovations* to be made when a completely new artifact is introduced. This translates to a random attachment event in the $N\to\infty$ limit. While this work does not generally use a network picture, it does translate directly into our network model (e.g., see [21]). Here the edges in our network realization represent the artifacts chosen by each individual. In cultural transmission problems, samples of these distributions are often available, from records of births, pedigree dog registrations, or reports from archaeological excavations [57].

It is relatively easy to see how the same model may be used for family names rather than the personal names of [22]. In this case the partners who change their family name are represented by the individual vertices, the family names are the artifact vertices and the edges represent the partners who keep their family name. This is then the constant population limit of the models in [26].

This family name example shows that this model may be linked to inheritance processes. As noted elsewhere [21–24] the oldest examples come from a simple model for the diversity of genes in a constant population due to Kimura and Crow [27,28]. In the case of a haploid cell (viruses, bacteria, and blue-green algae provide examples) the artifacts are alleles of a single gene carried by each individual. The preferential attachment events correspond to *inheritance* of genes.

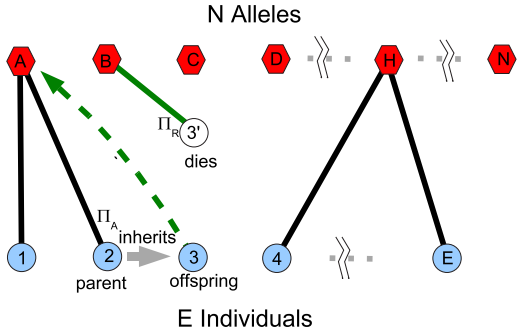

FIG. 12. (Color online) Interpretation of the example shown in Fig. 1 as a haploid gene inheritance and mutation model. Each individual carries one copy of a gene and each different version of the gene, an allele, is represented by an artifact vertex. The edges indicate the allele present in each individual. Note this also serves as a model of family names for a constant population if one partner inherits the family name of the other partner. In this case the alleles (artifacts) are the family names, the edges are the males, and the genes (individuals) are the females.

This produces a *drift* towards homogeneity and, if unchecked, a condensation or *fixation* in the frequency of alleles in the population. The random attachment process is *mutation* in this context.

In general a fitness is assigned to each gene representing the chance of survival and the successful birth rate associated with having that gene. There may also be different mutation rates associated with each gene. However, in the simplest models such factors are ignored. Translating the haploid gene model for a constant population into the language of our network rewiring model is then simple. The organisms are the individuals and we consider one gene carried by each individual. Each different allele of this gene is a distinct artifact vertex and so each edge records the allele carried by an individual. The rewiring example of Fig. 1 is translated into a haploid model as shown in Fig. 12.

In a diploid cell there are two copies of a gene and most cells of most higher organisms are of this type. Ignoring fitness, etc. we can see that we can represent the allele frequencies of one gene in a constant population of diploid cells with the usual rewiring model as shown in Fig. 13.

There is also a close relationship between our network model and various models of statistical physics, a connection already noted in some places [10,18]. In the original urn model of the Ehrenfests [58] one has E balls placed in two urns. At random times given by a Poisson process, a ball chosen at random is moved from one urn to another. This corresponds to a continuous time version of our model with the artifacts being the urns so $N=2$ and the individuals represent the balls. Choosing $p_r=1$ in our model reproduces the behavior of the original urn model.

There is one subtlety in that in the original urn model the ball is never put back into the urn it was drawn from. These events are allowed in our model and are precisely the ones which require the factors of $(1-\Pi)$ in our master equation (1) as they leave the configuration unchanged. The difference between the original urn model and our model for $N=2$, $p_r=1$ and continuous time is just a matter of a factor of 2 in the rates.

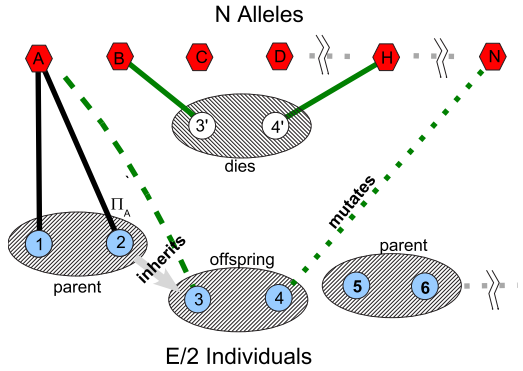

FIG. 13. (Color online) Interpretation of our model as a diploid gene inheritance and mutation model. Organism $(3',4')$ dies and is replaced by (3,4) whose parents are the organisms (1,2) and (5,6). From the (1,2) parent it inherits copy number 2 of the gene which is allele A. However, the gene it inherits from the (5,6) parent mutates to allele N.

However, generic urn models are often encountered in some obvious variations of the Ehrenfest version, in particular with N urns and with different forms for the rate at which balls are moved and where they are then placed [8–11]. Some of these variations of the original urn model are equivalent to other models such as the backgammon or balls-in-box models used for glasses [13,14], simplicial gravity [15], and wealth distributions [16]. The zero range processes [17–19] can also be interpreted as urn models, with the "misanthrope" process on a fully connected geometry being closest to our basic model.

Using the terminology of the urn model review [9], the "geometry" of the urn model refers to which urns are connected—an artifact network in our model as discussed in Sec. VI A. The simplest "mean-field" geometry, i.e., a complete graph for the artifact network, is what we assume in our simple model. On the other hand the basic zero-range process models [17,18] use a one-dimensional ring. If we allow processes where the ball is placed back into the urn it came from, then the rate at which a ball moves is given by $u(d,a)$ per ball where d is the departure urn and a the arrival urn. Usually the rates used factorize into two terms, one depending only on the number of balls in the departure urn k_d (number of edges, i.e., the artifact vertex degree) and the other on the number of balls in the arrival urn k_a. In our terminology $u(d,a)=\Pi_R(k_d)\Pi_A(k_a)$. Then the three rules for ball selection discussed in [8,9] correspond to our generalization (57) as follows: Rule A (random ball to random urn, Ehrenfest class) is our $q_p=1$, $p_r=1$; rule B (random urn to random urn, Monkey class) is our $q_a=1$, $p_r=1$; and rule C (random ball to random ball) is our $q_p=1$,$p_p=1$.

However, we stress that to include processes where balls are returned to the urn they were drawn from, the master equation has to contain the factors $(1-\Pi)$ while such terms are normally absent in the evolution equations of literature on urn and related models, e.g., in [8–10]. If we were to exclude such events then our transition rates $u(d,a)$ will not factorize into departure and arrival dependent terms [59]. For instance, in our language the factor normally associated with the arrival vertex, our attachment probabilities Π_A, will have to depend on the departure urn as well as on the properties of the arrival urn, and for us would take the form (59) while the literature usually uses simple factorizable forms, e.g., [8–11]. As we noted in Sec. VI A this will be important when a significant fraction of balls are in any one box, as is the case with a condensate.

There is a way around this problem and that is to work with our solution in continuous time (55) and then to rescale our time t back into the time t_{urn} of an urn model where one cannot put the ball back into the urn it was drawn from. From the number of these events allowed in our model but excluded from an urn model we have for infinitesimal time steps

$$dt - dt_{\text{urn}} = \left[\frac{p_r}{N} + \frac{p_p\langle k^2\rangle}{E\langle k\rangle}\right]dt, \tag{61}$$

where the second moment $\langle k^2\rangle$ is easily derived from $F_2(t)$ of Eq. (48).

Finally we note that many models in sociophysics may be cast as generalizations of our bipartite rewiring model. If we add an individual graph then for a copying (preferential attachment) event, an individual copies the artifact choice made by one of its neighbors in the individual graph. When $p_p=1$ and $N=2$ this is the basic Voter model [29], as used, for instance, for language evolution [31]. Our results are equivalent to having an individual graph which is complete with tadpoles [60]. Our time scale is $(\tau_2/E)=E/2$ which agrees with the $O(E)$ result quoted in [30]. However, our result shows the effect of adding some randomness to such Voter models on both the consensus and on the time scale to reach equilibrium.

Our results may also be useful in other sociophysics models. In one variation of the minority game [32] individuals choose the "best" strategy known to them, comparing their own against all those used by their neighbors as defined by an individual graph. Each artifact vertex in our model would then represent a different strategy. In this case what is best is continually changing as generally the more popular one strategy becomes the less successful it will be. Thus statistically, it is likely that the resulting instantaneous artifact degree distribution $n(k,t)$ will be indistinguishable from that obtained by just copying the artifact of a random neighbor which as a simple random walk is likely to lead to effective preferential attachment. It is no surprise then that the long time results for the popularity of strategies in [32] follows a simple inverse power law with a large degree cutoff, the form found in Eq. (35).

VII. SUMMARY AND CONCLUSIONS

The starting point of our work is the observation that the usual mean-field master equations seen for network evolution are not suitable for general rewiring problems. One needs to add the factors of $(1-\Pi)$ seen in Eq. (1) if the degree distribution is to behave properly at the maximum degree [37]. With these terms and the simplest case of linear attachment-removal probabilities the *exact* solution for the degree distribution at *any* time can be found for *arbitrary*

values of the parameters, here expressed in terms of the generating function $G(z,t)$ of Eqs. (5), (8), and (11). This is better than can be done for simple growing networks where the exact equilibrium solution is known for simple attachment probabilities but the finite size (finite time) system corrections are only known asymptotically (e.g., see [33,34,36]). Previous results for equivalent models give results that are only approximations, often for infinitely large systems in equilibrium though all are consistent with the results derived here [61]. We have also compared our analytic results against numerical simulation in several ways and seen that agreement is excellent. We know of no other network model that has the exact time dependent solution for arbitrary parameters and suggest that this model may prove to be as useful a model as the Erdős-Réyni random graph has been.

In particular the equilibrium degree distribution of [37] is found as the long time solution. It has two characteristic regimes: if when all edges have been rewired once (on average) at least one rewiring was done randomly then a simple inverse power law with exponential cutoff is obtained, otherwise we have a regime with a condensate.

We have confirmed the slow approach to equilibrium and the conjectured form for the second eigenvalue λ_1 of [38]. However, here we have shown that the long time evolution is governed not by the second largest eigenvalue but the third largest, $\lambda_2=1-(2p_r/E)-(2p_p/E^2)$ with associated time scale $\tau_2=-1/\ln(\lambda_2)$.

We have also noted that this simple bipartite graph rewiring model captures the degree distribution of many other networks, with that of the original Watts and Strogatz model [1] as one limit of our model. In particular we have the exact degree distribution at any time and any parameter value for the rewiring of a general random graph. From this we can obtain various global properties analytically as a function of time using various known formulas [53–56]. However, many of the alternative realizations require no explicit network as in the link to urn/backgammon/balls-in-boxes models and zero range processes [10–19].

The model also has a wide range of practical applications. As most practical systems can not grow indefinitely, this fixed sized rewiring model will often be more appropriate than a growing network model. The urn-type models have been applied to glasses [13], simplicial gravity [15], and wealth distributions [16]. Models for social science in both modern and archaeological contexts [20–24] can be cast as our model. The applications in these papers include baby name frequencies [22], pedigree dog breed popularity [23], and pottery styles [20,21]. Sociophysics models may also be related to our work. The Voter model [29,30], as applied to language evolution [31], and the choice of strategy in a minority game variant [32], may be linked to our bipartite graph approach. Finally basic models of population genetics [27,28] and more generally any process where inheritance is important, such as with family names [26], can be encoded by our network rewiring.

Many of the related examples in the literature also study cases beyond our simple model, for example nonlinear attachment probabilities $\Pi_A \propto k^\beta$ for $\beta \in \mathbb{R}$, attachment probabilities whose scale varies with the artifact (*fitness*), pure artifact or pure individual graphs, and growing systems $(dE/dt) \neq 0$. These can often be captured by extensions to our basic model but the downside of this sophistication is that the mean-field equations are then only approximations whose exact algebraic solution is probably unobtainable in any case. Rather the literature usually works in a large network long time approximation, $E \gg 1$, often in a particular part of parameter space such as $1 \gg p_r \gg E^{-1}$ or $p_r=0$. We though have exploited the simplicity of our model in order to obtain exact solutions for any time or parameter value.

At worst this simple bipartite model provides a useful null model against which to test other hypotheses [25]. However, we have also argued in Sec. VI A why copying may be a more widespread method than the obvious cases involving inheritance mechanisms.

Finally we note the scaling properties of the model. In many practical examples the artifacts are really categories imposed by investigators on a collection of objects. In almost all cases, each object could be individually identified if one wishes. Indeed the objects may be being chosen by individuals based on characteristics completely different from those recorded by the researcher. No pedigree dog [23] is genetically pure, a personal [22] or family name [26] may come in several close variations, and who assigns a particular style to an archaeological pottery find [20,21]?

Consider an exemplary small study [62] where the shoes of around 200 male physics students leaving a lecture were photographed. Various researchers categorized them in completely different ways giving different degree distributions from the same data. For instance, one could categorize each shoe by color, material, and fastening method. Still what constitutes say a "blue" shoe may be a context dependent matter of physical and social perception so researchers and wearers may not even agree how to classify a given shoe under the one scheme.

So if such artifact popularity distributions are to have much meaning they ought to be largely independent of this categorization. Thus consider pairing the artifacts at random and calculating the degree distribution for these pairs, $n_2(k)$, even though the model continues to make its rewiring selections based on the original single artifact vertices. That is at each event we choose to make a preferential (copying, inheritance) attachment or a random (innovation, mutation) attachment to the artifact pairs with exactly the same probability p_p and p_r. Given our *linear* attachment-removal probabilities the effective probability for attaching to a given artifact pair is just the sum of the degrees of its constituent artifacts, i.e., it is still proportional to the degree of the artifact pair. On the other hand the probability we attach to a given artifact chosen at random is halved but only because the number of artifact pairs N_2 is just half the original number of artifacts, $N \to N_2=N/2$. With the number of edges E unchanged, changing N to N_2 is the only change we need to make in our equations. Vitally, the form for the attachment and removal probabilities remains the same and thus the form of the solutions is unchanged. We will get the same qualitative behavior, a power law with an exponential cutoff. In such cases the cutoff ζ (28) remains unchanged and only the slope γ (26) changes in comparing $n(k)$ to the pair degree distribution $n_2(k)$. However, the slope is invariably indistinguishable from one in a practical data set or it will be un-

measurable with a small cutoff ζ. Thus for a linear attachment plus random attachment model, the distribution of artifact choice is independent of how artifacts are classified for all practical purposes.

ACKNOWLEDGMENT

T.S.E. thanks H. Morgan and W. Swanell for useful conversations.

[1] D. J. Watts and S. H. Strogatz, Nature (London) **393**, 440 (1998).
[2] Z. Burda, J. D. Correia, and A. Krzywicki, Phys. Rev. E **64**, 046118 (2001).
[3] S. N. Dorogovtsev and J. F. F. Mendes, *Evolution of Networks: From Biological Nets to the Internet and WWW* (Oxford University Press, Oxford, 2003).
[4] S. N. Dorogovtsev, J. F. F. Mendes, and A. Samukhin, Nucl. Phys. B **666**, 396 (2003).
[5] K. Park, Y.-C. Lai, and N. Ye, Phys. Rev. E **72**, 026131 (2005).
[6] Y.-B. Xie, T. Zhou, and B-.H. Wang, e-print arXiv:cond-mat/0512485.
[7] J. Ohkubo, K. Tanaka, and T. Horiguchi, Phys. Rev. E **72**, 036120 (2005).
[8] C. Godrèche, J. P. Bouchaud, and M. Mézard, J. Phys. A **28**, L603 (1995).
[9] C. Godrèche and J. M. Luck, J. Phys.: Condens. Matter **14**, 1601 (2002).
[10] J. Ohkubo, M. Yasuda, and K. Tanaka, Phys. Rev. E **72**, 065104(R) (2005).
[11] J. Ohkubo, M. Yasuda, and K. Tanaka, J. Phys. Soc. Jpn. **75**, 074802 (2006).
[12] P. Bialas, L. Bogacz, Z. Burda, and D. Johnston, Nucl. Phys. B **575**, 599 (2000).
[13] F. Ritort, Phys. Rev. Lett. **75**, 1190 (1995).
[14] P. Bialas, Z. Burda, and D. Johnston, Nucl. Phys. B **493**, 505 (1997).
[15] P. Bialas, Z. Burda, and D. Johnston, Nucl. Phys. B **542**, 413 (1999).
[16] Z. Burda, D. Johnston, J. Jurkiewicz, M. Kaminski, M. A. Nowak, G. Papp, and I. Zahed, Phys. Rev. E **65**, 026102 (2002).
[17] M. R. Evans, Braz. J. Phys. **30**, 42 (2000).
[18] M. R. Evans and T. Hanney, J. Phys. A **38**, R195 (2005).
[19] O. Pulkkinen and J. Merikoski, J. Stat. Phys. **119**, 881 (2005).
[20] F. D. Neiman, Am. Antiq. **60**, 1 (1995).
[21] R. A. Bentley and S. J. Shennan, Am. Antiq. **68**, 459 (2003).
[22] M. W. Hahn and R. A. Bentley, Proc. R. Soc. London, Ser. B **270**, S120 (2003).
[23] H. A. Herzog, R. A. Bentley, and M. W. Hahn, Proc. R. Soc. London, Ser. B **271**, S353 (2004).
[24] R. A. Bentley, M. W. Hahn, and S. J. Shennan, Proc. R. Soc. London, Ser. B **271**, 1443 (2004).
[25] R. A. Bentley and S. J. Shennan, Science **309**, 877 (2005).
[26] D. Zanette and S. Manrubia, Physica A **295**, 1 (2001).
[27] M. Kimura and J. F. Crow, Genetics **49**, 725 (1964).
[28] J. F. Crow and M. Kimura, *An Introduction to Population Genetics Theory* (Harper and Row, New York, 1970).
[29] T. M. Liggett, *Interacting Particle Systems* (Springer-Verlag, New York, 1985).
[30] V. Sood and S. Redner, Phys. Rev. Lett. **94**, 178701 (2005).
[31] D. Stauffer, X. Castello, V. M. Eguiluz, and M. San Miguel, Physica A **374**, 835 (2006).
[32] M. Anghel, Z. Toroczkai, K. E. Bassler, and G. Korniss, Phys. Rev. Lett. **92**, 058701 (2004).
[33] S. N. Dorogovtsev and J. F. F. Mendes, Adv. Phys. **51**, 1079 (2002).
[34] P. L. Krapivsky and S. Redner, Phys. Rev. E **63**, 066123 (2001).
[35] P. L. Krapivsky and S. Redner, J. Phys. A **35**, 9517 (2002).
[36] T. S. Evans and J. P. Saramäki, Phys. Rev. E **72**, 026138 (2005).
[37] T. S. Evans, Eur. Phys. J. B **56**, 65 (2007).
[38] T. S. Evans and A. D. K. Plato, e-print arXiv:physics/0608052, Proceedings of ECCS06 (to be published).
[39] Alternatively the order in which each individual changes their choice could be made in a more systematic way, either in a fixed order or a random order changed once each individual has been rewired once. There could even be changes at the same time, the model used in [21–24]. We have tried these variations numerically and they appear to make little difference to the equilibrium results.
[40] The physical time $\mathcal{T}$ of each event $t \in \mathbb{Z}$ should be monotonically increasing $\mathcal{T}(t+1) > \mathcal{T}(t)$ but otherwise it can be arbitrary. This relationship should be derived from the actual frequency of changes in the problem of interest.
[41] Alternatively we also have models where the process chooses an edge or artifact directly, with the probability Π_R. The distinction is immaterial for the degree distribution of the artifacts so we shall take these alternatives for granted.
[42] These are the "safe situations" of large graphs discussed in Chap. 4 of [3].
[43] In this paper "random" without further qualification indicates that a uniform distribution is used to draw from the set implicit from the context.
[44] J. Saramäki and K. Kaski, Physica A **341**, 80 (2004).
[45] We have chosen to normalize the eigenfunctions such that $\omega^{(m)}(k=0)=1$. The physical normalization needed in the problem is contained in the c_m coefficients of Eq. (8).
[46] The only case of eigenvalue crossing occurs at $p_r=0$ when there is degeneracy in the two largest eigenvalues with $1=\lambda_0=\lambda_1$.
[47] P. L. Krapivsky, S. Redner, and F. Leyvraz, Phys. Rev. Lett. **85**, 4629 (2000).
[48] In this $p_r=0$ limit we have degeneracy between eigenfunctions number zero and one. However, we will see below that eigenfunction one $\omega^{(1)}$ does not contribute to any physical solution so there is no ambiguity about our solution in this case.
[49] This means that the generating function may be written as $G(z)=\Sigma_{n=0}^{E}(z-1)^n \binom{E}{n} F_n$, a form useful when solving the differential equation (9).

[50] A tadpole in a general graph is an edge starting and ending at the same vertex. For example, see vertex A in Fig. 10.
[51] A. Vázquez, e-print arXiv:cond-mat/0006132.
[52] A. Vázquez, Phys. Rev. E **67**, 056104 (2003).
[53] M. Molloy and B. Reed, Random Struct. Algorithms **6**, 161 (1995).
[54] M. Molloy and B. Reed, Combinatorics, Probab. Comput. **7**, 295 (1998).
[55] M. E. J. Newman, S. H. Strogatz, and D. J. Watts, Phys. Rev. E **64**, 026118 (2001).
[56] S. N. Dorogovtsev, J. F. F. Mendes, and A. Samukhin, Nucl. Phys. B **653**, 307 (2003).
[57] Sometimes these samples are medium term time averages of the degree distribution $\int p(k,t)$ and such distributions may take a different form, a problem addressed in [22,23].
[58] P. Ehrenfest and T. Ehrenfest, Phys. Z. **8**, 311 (1907).
[59] One exception is for a two urn model as then the number of balls in the arrival urn may always be written in terms of those in the departure urn and vice versa. This means typical expressions for rates are always factorizable.
[60] If this is performed on just a complete graph then this is an $N=2$ urn model with rule C of [8,9] performed on mean-field urn geometry.
[61] The literature does, however, tackle other more complicated variations of the model not considered here.
[62] H. Morgan and W. Swanell, Imperial College London BSc project reports, 2006 (unpublished).